Mixed-Layer Shear Generated by Wind Stress in the Central Equatorial Pacific*

FERNANDO SANTIAGO-MANDUJANO AND ERIC FIRING

Joint Institute for Marine and Atmospheric Research, University of Hawaii at Manoa, Honolulu, Hawaii

(Manuscript received 17 April 1989, in final form 19 March 1990)

ABSTRACT

Sixteen months of wind and current profile observations in the central equatorial Pacific show the response of the upper-ocean shear to local wind forcing. The shear at the ocean surface is significantly correlated with the wind stress in direction but not in magnitude, implying that the vertical eddy viscosity coefficient is proportional to the square of the wind speed or to the stress. Using this variable eddy viscosity coefficient in Stommel's model of the Equatorial Undercurrent, we calculate shears in the mixed layer that compare well with the observations. The flow is downwind on the equator and tends toward an Ekman spiral off the equator.

1. Introduction

Studies in the equatorial Pacific have shown variable wind-driven shear flows in the nearly homogeneous surface layer. In the western Pacific, current profile sections have shown that the usual westward south equatorial current is sometimes replaced by eastward equatorial flows in the top 100 m, apparently in response to prior westerly winds (Hisard et al. 1970; Colin et al. 1973; Jarrige and Rual 1981). Similarly, moored current measurements at 165°E have shown an eastward current in the upper 125 m generated by a westerly wind burst (McPhaden et al. 1988). In the central Pacific, moored current and wind records from the NORPAX Tahiti Shuttle Experiment (Wyrtki et al. 1981) show high correlation between variations in local winds and currents at 15 m, whereas currents at 100 m were relatively steady. In the eastern Pacific, much of the complicated structure in the top 50 m of velocity profile sections across the equator has been attributed to local wind forcing (Leetmaa and Wilson 1985).

Attempts to model wind-generated shear usually use the concept of a vertical eddy viscosity, but it is not clear how large the coefficient, A_v, should be (Table 1) or how it should be parameterized. The Richardson number parameterization proposed by Pacanowski and Philander (1981) for numerical modeling seems to be a considerable improvement over a constant A_v and is conceptually consistent with observations of turbulent dissipation versus Richardson number (Peters et al. 1988). Ekman (1905) proposed an entirely different parameterization; observations of the relationship between surface drift and wind (in the tropical Atlantic and under the ice in the Arctic) led him to propose that in the mixed layer A_v is proportional to the square of the wind speed. We will show evidence that this relationship also holds within 3° lat. of the equator in the central Pacific.

Stommel (1960) developed the simplest useful model of wind-driven shear flows near the equator. A time-dependent extension of this model (Moore 1979) was used by McPhaden et al. (1988) to calculate the vertical eddy viscosity coefficient in the mixed layer of the western equatorial Pacific from the change in shear associated with a westerly wind burst. Based on the time lag between the wind and the shear (between 10 and 100 m), they inferred an eddy viscosity of $18.3 \times 10^{-3}\,m^2\,s^{-1}$, and from the correlation between wind stress and shear during a single month (May 1986) they calculated an eddy viscosity of $9.8 \times 10^{-3}\,m^2\,s^{-1}$. Repeating the regression calculation for a longer period (January–July 1986), they found a low correlation coefficient (0.23) and a much smaller eddy viscosity, $1.0 \times 10^{-3}\,m^2\,s^{-1}$. Because data were available only from an equatorial mooring with rather coarse vertical resolution, neither the variation of the shear with depth nor with latitude could be compared with the model.

Here we investigate the relationship between local winds and upper ocean shear in a 16-month time series including 41 cross-equatorial sections, 3°S to 3°N, and spanning a period of major wind changes: the 1982–83 El Niño. This dataset lacks the temporal resolution required by the time-dependent model, so we compare our observations with hindcasts from the quasi-steady Stommel model instead. The main features of the model, anticyclonic rotation and decay of the shear with depth, are indeed found in the observations.

* Hawaii Institute of Geophysics contribution 2330 and Joint Institute for Marine and Atmospheric Research contribution 90-231.

Corresponding author address: Dr. Eric Firing, JIMAR, 1000 Pope Road, University of Hawaii, Honolulu, HI 96822.

TABLE 1. Eddy viscosity coefficient estimates (A_v) from upper ocean observations.

Author	A_v (10^{-3} m^2 s^{-1})	Method	Location
Hidaka and Momoi (1961)	1.0–2.0	Ekman layer compared with wind stress and surface current data.	Tropical Pacific
Jones (1973)	3.9	Calculated A_v as function of Richardson No. assuming a logarithmic velocity profile; used measurements of current shear, temperature, and salinity.	Equatorial Pacific undercurrent
Smith (1974)	4.0	High-resolution current meter measurements of Reynolds stresses.	Arctic Ocean
Halpern (1974)	0.1–11.4	Ekman layer theory compared with moored wind and current observations.	Northeastern Pacific
Halpern (1976)	5.5	Same as in Halpern (1974).	Coast of Oregon
Halpern (1977)	12.5	Balance between surface shear and wind stress; moored wind and current data.	Northwest Africa
Kase and Olbers (1979)	3.0	Time-dependent Ekman model applied to inertial waves.	Atlantic equatorial countercurrent
Halpern (1980)	5.6	Same as in Halpern (1977).	Atlantic equatorial countercurrent
Crawford and Osborn (1981)	1.0	Dissipation method; measured turbulent dissipation and undercurrent shear.	Central equatorial Pacific
Gregg et al. (1985)	2.0	Same as in Crawford and Osborn (1981)	Central equatorial Pacific
Peters et al. (1988)	5.0	Same as in Crawford and Osborn (1981)	Central equatorial Pacific
McPhaden et al. (1988)	1.0–18.0	Time-dependent Ekman layer; moored wind and current data.	Western equatorial Pacific

2. Data and methods

During March 1982 through June 1983, as part of the Pacific Equatorial Ocean Dynamics project (PEQUOD), 21 cruises were made in the central equatorial Pacific (Firing 1987). Profiles of absolute current velocity and temperature together with shipboard wind observations were obtained every half degree from 3°N to 3°S along 159°W (Fig. 1).

Current velocities and temperatures were sampled at about 8-m vertical intervals using the Pegasus acoustic dropsonde (Spain et al. 1981). The surface velocity was taken as the average drift of the Pegasus before recovery, an interval ranging from a few minutes to an hour. Descending and ascending Pegasus profiles were combined and a parabola was fit to the top ten points, or about 40 m. The surface velocity was given extra weight. The vertical shear of the horizontal currents at the surface was the first derivative of this parabola at 0 m.

The surface drift velocity of the Pegasus may have been contaminated by wave rectification, although the characteristics of the Pegasus (spherical, and almost neutrally buoyant) were such as to minimize the downwind drift (Niiler et al. 1987). To test the importance of the surface observation in our results, the correlation between wind stress and surface shear directions (section 3) was recalculated with the surface point omitted from the shear estimate. The resulting correlation was reduced but was still significant at the 95% confidence level, indicating that the surface drift was not essential to the analysis.

The study was restricted to the 358 profiles with mixed layers deeper than 40 m; the base of the mixed layer was defined as the shallowest point where the vertical temperature gradient exceeded 0.05°C m^{-1}. Mixed layer depth varied greatly from profile to profile (Fig. 2); averaged over each cruise, it stayed near 100

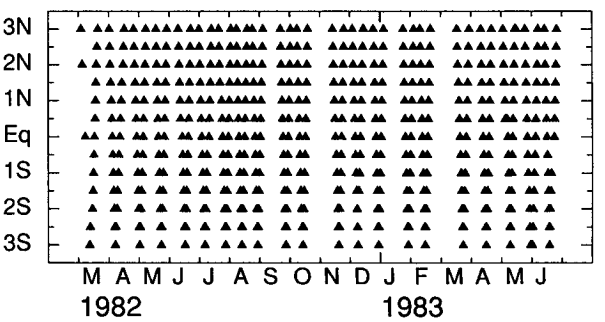

FIG. 1. Location of the stations along 159°W during the PEQUOD program.

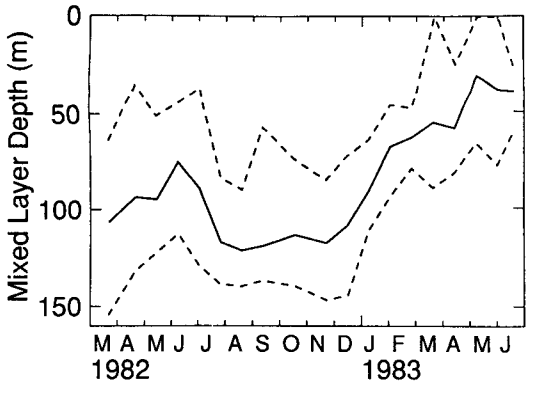

FIG. 2. Mixed-layer depth during the PEQUOD period averaged in each of 20 time bins regardless of latitude (solid line), and the extrema for each bin (dashed lines).

m during the first 12 months and then decreased to about 40 m by the end of the project. A diurnal cycle in both the mixed layer depth and the shear was evident in this dataset; a similar diurnal cycle in the mixed layer depth has been found previously in the same region (Schneider and Müller 1990).

To estimate the error in the surface shear, we first placed upper bounds on the horizontal velocity error and the vertical position error, calculating both from the profiles themselves. When the Pegasus is drifting on the surface, the standard deviation of its velocity has three sources: position errors, short-term velocity variations from the surface wave field, and longer term variations from the small-scale variability of the currents. The surface velocity standard deviation is, therefore, an upper bound estimate of the horizontal velocity uncertainty in the mixed layer. Using drifts when wind speeds were below 3 m s^{-1} yielded a standard deviation of 0.04 m s^{-1}. This corresponds to a standard deviation of 0.5 m in the horizontal Pegasus position (measured every 16 s). Variations in the measured vertical velocity reflect actual irregularities in the fall rate plus errors in the vertical position calculated from the pressure. In the top 80 m, the vertical velocity standard deviation was 0.02 m s^{-1}, equivalent to an upper bound estimate of 0.2 m for the vertical position standard error. These horizontal velocity and vertical position errors were then used with a simple velocity profile (with vertical shear decreasing from 0.025 s^{-1} at the surface to 0.003 s^{-1} at 60 m) in a Monte Carlo experiment. The resultant surface shear standard deviation was 0.0035 s^{-1}. This upper bound estimate is closer than we would like to the mean measured surface shear magnitude, 0.01 s^{-1}, but not so close as to render the data useless.

The wind stress was assumed proportional to the wind speed squared: $\boldsymbol{\tau} = \rho_a C_D |\mathbf{U}| \mathbf{U}$ with ρ_a, the air density, $\mathbf{U}$ the wind velocity vector at 10 m above the sea surface, and C_D the drag coefficient. Here, C_D was considered constant ($C_D = 1.14 \times 10^{-3}$; Large and Pond 1982) because only wind speeds less than 10 m s^{-1} were included in the study.

Confidence limits for correlation analysis were obtained by estimating the integral time scale from the respective time series and the corresponding equivalent degrees of freedom (Davis 1976, 1977).

3. Correlation between surface shear and wind stress

Because stress is a function of shear and must be continuous across the air–sea interface, one would expect a high correlation between the wind stress and the shear just below the surface. We find that the directions of these two vectors were indeed highly correlated (significant at the 99% confidence level, Fig. 3a). Their

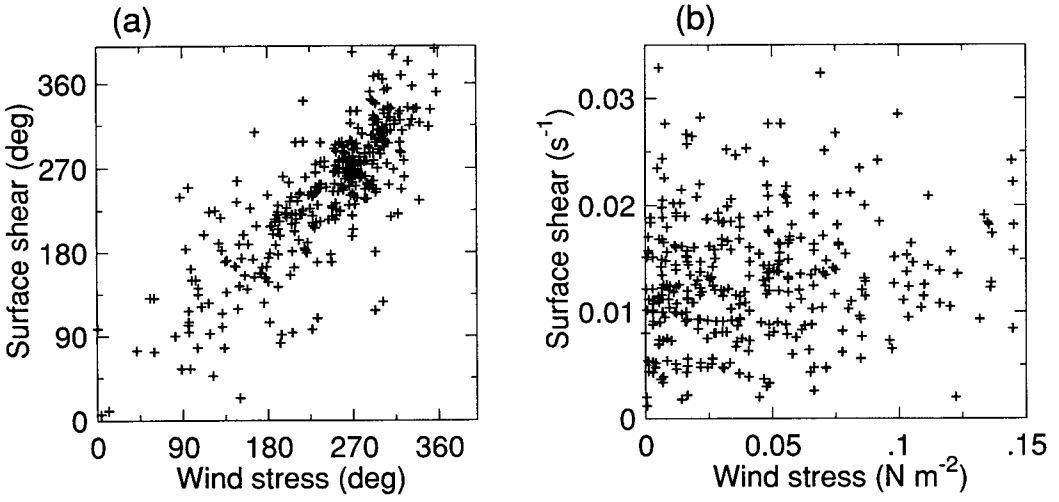

FIG. 3. Surface shear vs wind stress directions (a) and magnitudes (b) from all profiles, regardless of latitude (358 data pairs). The directions increase clockwise from true North. The correlation coefficient for directions is 0.8, significantly different from zero. Magnitudes are uncorrelated.

magnitudes, however, were not significantly correlated (Fig. 3b). The absence of correlation in magnitude has important consequences for the eddy viscosity coefficient (A_v), defined by the relation:

$$A_v \mathbf{u}_z = \boldsymbol{\tau}/\rho = \rho_a C_D \mathbf{U}|\mathbf{U}|/\rho, \qquad (1)$$

with ρ the density of water and $\mathbf{u}_z$ the surface shear vector. If the surface shear magnitude is independent of the wind speed, then A_v must be proportional to the square of the wind speed. This proportionality was confirmed by the following alternative analysis, involving the Cartesian rather than the polar components of the vectors.

Values for A_v as a function of wind speed were calculated from each component of (1) by linear regression. Data were grouped by wind speeds in adjacent intervals centered at 1.25, 2.5, 3.5, 4.5, 5.5, 6.5, 7.5 and 9 m s^{-1}. Correlations between colinear components of surface shear and surface stress were significant at the 95% level in all but three of the cases. (The correlation of the meridional components at 1.25 and 6.5 m s^{-1} were significant at the 90% level, and the zonal component correlation at 1.25 m s^{-1} was not significant.) Regression of the logarithm of A_v (m^2 s^{-1}) against the logarithm of the wind speed U (m s^{-1}) gives (Fig. 4)

$$A_v = a(U/U_0)^b, \quad 1 \text{ m s}^{-1} < U < 10 \text{ m s}^{-1} \qquad (2)$$

with $U_0 = 1.0$ m s^{-1}, $a = 8 \times 10^{-5}$ m^2 s^{-1} and $b = 2.2$. This shows A_v varying nearly as the square of the wind speed. The best quadratic fit, also shown for comparison in Fig. 4, is

$$A_v = cU^2; \quad c = 1.2 \times 10^{-4} \text{ s}. \qquad (3)$$

This implies that any approximation of A_v (or of eddy diffusivity) in the mixed layer as constant in time can be valid only if the wind speed is also nearly constant.

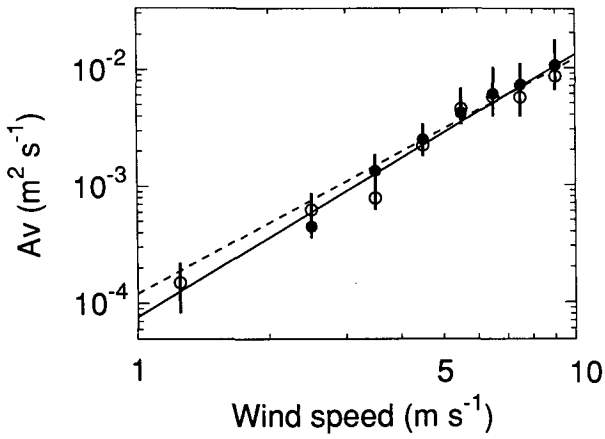

FIG. 4. Vertical eddy viscosity coefficient (A_v) as a function of wind speed (U) calculated from the zonal velocity component (full circles) and the meridional velocity component (open circles). Vertical bars show the 95% confidence limits. The solid line is the linear regression of logA_v against log$U$ and the dotted line is the best fit to $A_v = cU^2$.

4. Variation of the shear vector with depth

Our calculation of A_v uses the colinear components of wind stress and our estimate of surface shear, which were significantly correlated. The cross components were not significantly correlated; as required by (1), the surface shear was found to be in the direction of the wind stress.

Off the equator we expect the shear vector to rotate with depth in an Ekman layer. Because the correlation between wind stress and current shear may be reduced by unresolved variability in the wind field, we are prompted to directly estimate the rotation of the shear vector with depth, regardless of the wind. Let $U \equiv u + iv$ be the complex representation of the velocity vector from a single descending or ascending profile. We then find the least-squares fit of a parabola centered at $z_0 = 20$ m to the top five observations (about 40 m) within the mixed layer of this profile:

$$U(z) \approx U_0 + U_0'(z - z_0) + \tfrac{1}{2}\gamma U_0'(z - z_0)^2,$$

where primes denote differentiation, the subscript zero indicates evaluation at z_0, and $\gamma \equiv U_0''/U_0'$. For $|\gamma(z - z_0)| \ll 1$, the shear can be approximated as an exponential function of depth:

$$U'(z) \approx U_0' e^{\gamma(z - z_0)}.$$

The rotation rate of the shear vector with depth is the imaginary part of γ, $\Im(\gamma)$, with positive values indicating clockwise rotation with increasing depth. The variation with depth of shear magnitude is the real part of γ, $\Re(\gamma)$, positive values indicating shear decay with depth.

The mean value of $\Im(\gamma)$ over all profiles at each latitude is positive north of the equator and negative south of the equator, consistent with Ekman turning (Fig. 5a). Typical values are one degree of rotation per meter of depth. The statistical significance is marginal, however. Many of the means differ from zero by less than two standard errors (calculated assuming all profiles at a given latitude are independent). In addition, rotation of the shear vector in the same direction as the Ekman spiral can be caused by inertial motions with downward group velocity (Leaman and Sanford 1975). This was not the dominant cause of rotation in the present dataset, however, as the rotations of the time-mean velocity vectors at each latitude (not shown) were similar to the mean rotations in Fig. 5a. The mean values of $\Re(\gamma)$ at each latitude are positive in all cases (Fig. 5b) with typical values of 0.03 m^{-1}, indicating a shear decay with increasing depth of about 3% per meter.

The observed correlation between wind and shear, the anticyclonic rotation of the current with depth, and

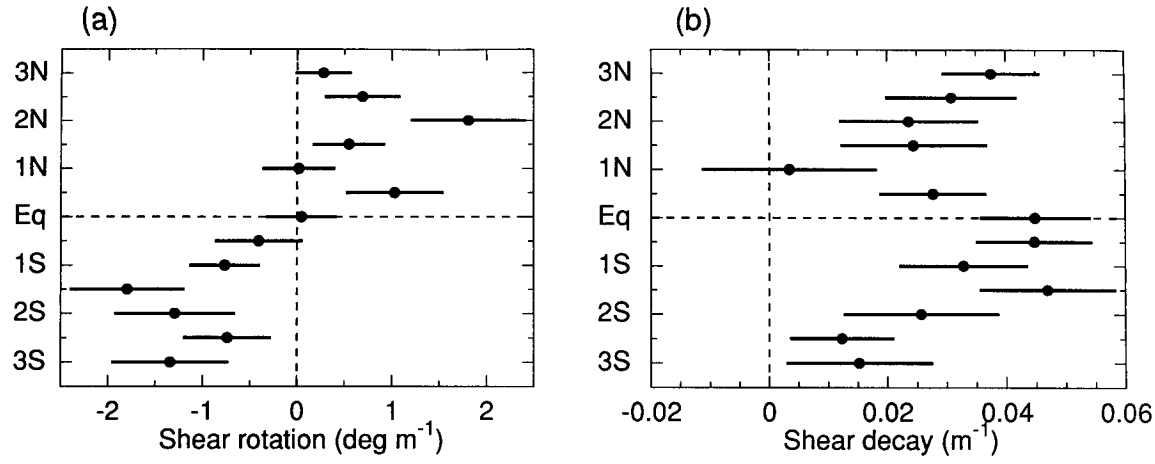

FIG. 5. Variation of the shear vector with depth at 20 m, calculated by least-squares fit of data from 0–40 m: (a) rotation, positive for clockwise turning with increasing depth; (b) magnitude trend, positive for magnitude decreasing with depth. Error bars are ±1 standard error of the mean.

the shear decay are consistent with Ekman layer dynamics. The simplest model of Ekman dynamics near the equator is that of Stommel (1960). In the next section Stommel's model is used to hindcast the shear generated from the observed winds, for comparison with the observed shear.

5. Comparison with Stommel's model

Stommel's (1960) model was originally applied to the Equatorial Undercurrent but is actually better suited to the study of shear in the mixed layer (Moore 1979; McCreary 1985). The model assumes steady linear flow in a homogeneous surface layer driven by the wind stress. There is a free-slip boundary condition at the bottom of the layer, and horizontal friction is neglected. The result is a parabolic downwind velocity profile on the equator, blending smoothly into a surface Ekman layer far from the equator. There are two free parameters: A_v and the mixed layer depth.

Using A_v given by (2) and with a mixed layer depth defined as before (section 2), the model was used to hindcast the observed profiles. The effect of error in the Pegasus measurements was simulated by adding Gaussian random noise of 0.04 m s^{-1} to each velocity point. To provide stable statistics, the mean and standard deviation were calculated for each latitude, with 100 realizations of each simulated profile. The simulated standard error of the mean was then the simulated standard deviation divided by the square root of the number of observed profiles at each latitude.

The modeled shear rotation (Fig. 6a) is similar in sign and magnitude to the observed (Fig. 5a). Typical values are about one degree of rotation per meter. Shear amplitude (Fig. 6b) decreases with depth at all latitudes at rates near 0.03 m^{-1}, again similar to the observed (Fig. 5b). The decay is generally more rapid away from the equator in the model but not in the observations. The simulated standard errors of the mean are also quite similar to those from the observations and several times larger than in a simulation with zero velocity error (not shown). This suggests that errors in the shear measurement by the Pegasus are contributing substantially to the differences between the observed and modeled shears, and to the scatter evident in Figs. 3 and 5. Measurement errors, however, do not appear to account for differences such as the observed low rate of rotation at 3°N and high shear decay rate at the equator.

6. Discussion

In this study we have investigated the relationship between the wind stress and the vertical shear of the horizontal currents in the equatorial mixed layer by analyzing a 16-month time series of current observations that included 41 cross-equatorial sections in the central Pacific. The surface shear is correlated with the local wind in direction but not in magnitude, implying that the vertical eddy viscosity coefficient is proportional to the square of the wind speed or to the wind stress (3). This simple relationship begs for a simple explanation, and we regret that we have none to offer.

Ekman (1905) derived (3) from his Ekman layer equations plus admittedly weak observational evidence that the ratio of wind speed U to wind-induced surface current u is roughly constant for any given latitude, ϕ: $u = 0.0127U(\sin\phi)^{-1/2}$. Combined with the quadratic relation between wind speed and stress, this led to the conclusion that the Ekman depth D = (7.6 s) $\times U(\sin\phi)^{-1/2}$ and $A_v = cU^2$. Hence, as the wind speed increases, both the surface current and the depth of the boundary layer increase proportionately, keeping their ratio, and the shear, constant. Near the equator the mixed layer depth, not the Ekman depth, limits the boundary layer thickness, but we did not find any

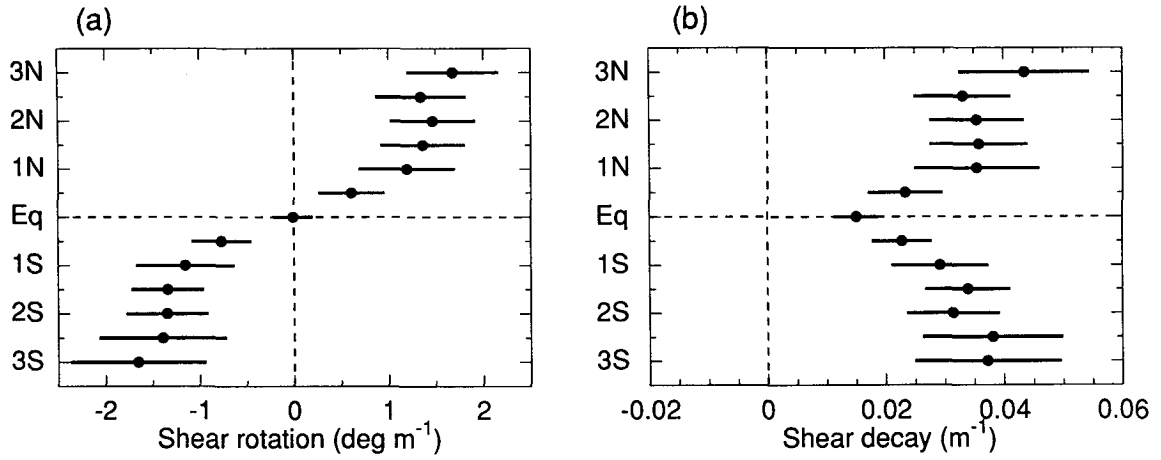

FIG. 6. As in Fig. 5 but hindcast using the Stommel model. The error bars, ±1 standard error of the mean, are based on a random error of 0.04 m s^{-1} standard deviation added to the modeled velocities.

correlation between the wind speed and the mixed-layer depth in the PEQUOD profiles. Therefore, if (3) is generally valid in the equatorial oceans, it may be for different reasons than at higher latitudes. It is also possible that (3) actually is not a good parameterization for higher latitudes. Based on observations of surface currents and winds, Thorade (1914) proposed that for wind speeds below 6 m s^{-1}, (3) should be replaced by $A_v = dU^3$ with $d = 1.02 \times 10^{-4}$ s^2 m^{-1}. We are aware of no more modern investigation of such parameterizations, with the partial exception of Halpern (1974).

Our constant of proportionality between A_v and U^2, $c = 1.2 \times 10^{-4}$ s, is smaller than previous estimates. Ekman (1905) found $c = 4 \times 10^{-4}$ s. More recently, Halpern (1974), using surface current and wind observations from the North Pacific during the passage of a storm, found a mean ratio of near-surface current to wind speed consistent with $c = 4.3 \times 10^{-4}$ s, almost identical to Ekman's (1905) value but a factor of 3.6 larger than found in the present study. Halpern took this value of c as the upper bound for a mixed layer and supposed that it was reduced by a function of the Richardson number in stratified regions. Hence, the weak but stable stratification usually found in the equatorial surface layer could account for our lower value of c. It is not clear, however, that the Richardson number is the correct parameter for taking stratification into account very near the ocean surface. Shear flow instability is not the only source of turbulent energy; surface wave breaking and convection (even if only during nocturnal cooling; Moum and Caldwell 1985; Peters et al. 1988) may play important roles.

There is some evidence at midlatitudes for a logarithmic boundary layer in the top 5 m of the mixed layer (Richman et al. 1987). In a 6-day record of currents measured from a drifting current meter string, the shear between 2.5 and 5.5 m was proportional to the friction velocity (which is proportional to the wind speed). For two reasons this is not necessarily inconsistent with our results: (i) we do not resolve shear over such a small vertical interval but estimate surface shear from a parabola fit to velocity measurements from the top 40 m; and (ii) coherence at the high frequencies resolved by Richman et al. (1987) could be swamped by incoherence at the lower frequencies present in our 16-month ensemble of profiles.

With a stress-dependent eddy viscosity coefficient and observed mixed layer depths, the Stommel (1960) equatorial undercurrent model produced mixed-layer shears similar to those observed. The main features are downwind flow on the equator, anticyclonic rotation off the equator, and decreasing shear with depth. We are not surprised to observe these features but are pleased that they appear in the Pegasus dataset despite its limitations in temporal and vertical resolution and in accuracy. Because of these limitations we have considered only the first derivative of shear with depth and have assumed the eddy viscosity coefficient is constant within the mixed layer. This may be a poor approximation but its simplicity is appropriate for the coarse vertical resolution of the data.

The sampling schedule, with sections at roughly 1.5-week intervals, was inadequate to resolve much of the temporal variability. The shear probably could be hindcast more accurately with a time-dependent model that integrates the effect of winds a few days prior to each current profile. McCreary (1985) calculated an adjustment time scale of six days for a time-dependent equatorial mixed-layer model. McPhaden et al. (1988), using moored observations of currents and winds at 165°E, found an e-folding time scale of about one day for the adjustment of the mixed-layer shear to a westerly wind burst.

The present work neglects density stratification in the upper ocean because there were no salinity measurements. Experiments to refine our results ideally

should include moored or drifting wind, current, temperature, salinity, microstructure and air–sea flux measurements. It should then be possible to study A_v as a function of wind speed, buoyancy flux, stratification, depth and the large-scale vertical shear structure.

Acknowledgments. This research was funded by the National Science Foundation under Grant OCE83-14486 of the PEQUOD program. During the completion of this research one author (F S-M) was partially supported by a CONACYT fellowship from the government of Mexico. We thank Peter Müller and Dennis Moore for helpful discussions and two anonymous reviewers for their comments that led to major revision of this manuscript.

REFERENCES

Colin, C., F. Jarrige, F. Rougerie and P. Rual, 1973: Equatorial current systems north of New Guinea. *Kuroshio, 3, Proc. of the Third CSK Symp.*, Bangkok, 1972, 150–160.

Crawford, W. R., and T. R. Osborn, 1981: Control of equatorial ocean currents by turbulent dissipation. *Science,* **212,** 539–540.

Davis, R. E., 1976: Predictability of sea surface temperature and sea level pressure anomalies of the North Pacific. *J. Phys. Oceanogr.,* **6,** 249–266.

——, 1977: Techniques for statistical analysis and prediction of geophysical fluid systems. *Geophys. Astrophys. Fluid Dyn.,* **8,** 245–277.

Ekman, V. W., 1905: On the influence of the earth's rotation on ocean currents. *Ark. f. Mat. Astr. och Fysik. k. Sv. Vet. Ak., Stockholm,* **2,** 53 pp.

Firing, E., 1987: Deep zonal currents in the central equatorial Pacific. *J. Mar. Res.,* **45,** 791–812.

Gregg, M. C., H. Peters, J. C. Wesson, N. S. Oakey and T. J. Shay, 1985: Intensive measurements of turbulence and shear in the equatorial undercurrent. *Nature,* **318,** 140–144.

Halpern, D., 1974: Observations of the deepening of the wind-mixed layer in the northeast Pacific Ocean. *J. Phys. Oceanogr.,* **4,** 454–466.

——, 1976: Structure of a coastal upwelling event observed off Oregon during July 1973. *Deep-Sea Res.,* **23,** 495–508.

——, 1977: Description of wind and upper ocean current and temperature variations on the continental shelf off northwest Africa during March and April 1974. *J. Phys. Oceanogr.,* **7,** 422–430.

——, 1980: Variability of near-surface currents in the Atlantic north equatorial countercurrent during GATE. *J. Phys. Oceanogr.,* **10,** 1213–1220.

Hidaka, K., and T. Momoi, 1961: Determination of the vertical eddy viscosity in sea water from wind stresses and surface current velocities. *Rec. Oceanogr. Works Japan* **6,** 1–10.

Hisard, P., J. Merle and B. Voituriez, 1970: The equatorial undercurrent at 170°E in March and April 1967. *J. Mar. Res.,* **28,** 281–303.

Jarrige, F., and P. Rual, 1981: Measurements in the equatorial current of the Atlantic and Pacific oceans. *Recent Progress in Equatorial Oceanography: A report of the final meeting of SCOR Working Group 47 in Venice, Italy.* J. P. McCreary, Jr., D. W. Moore and J. M. Witte, Eds., Nova University/N.Y.I.T. Press, 111–120.

Jones, J. A., 1973: Vertical mixing in the Equatorial Undercurrent. *J. Phys. Oceanogr.,* **3,** 286–296.

Kase, R. H., and D. J. Olbers, 1979: Wind-driven inertial waves observed during Phase III of GATE. *Deep-Sea Res.,* **26**(Suppl., Part A), 191–216.

Large, W. G., and S. Pond, 1982: Sensible and latent heat flux measurements over the Ocean. *J. Phys. Oceanogr.,* **12,** 464–482.

Leaman, K. D., and T. B. Sanford, 1975: Vertical energy propagation of internal waves; a vector spectral analysis of velocity profiles. *J. Geophys. Res.,* **80,** 1,975–1,978.

Leetmaa, A., and D. Wilson, 1985: Characteristics of near surface circulation patterns in the eastern equatorial Pacific. *Progress in Oceanography,* Vol. 14, Pergamon, 339–352.

McCreary, J. P., 1985: Modeling equatorial ocean circulation. *Ann. Rev. Fluid Mech.,* **17,** 359–409.

McPhaden, M. J., H. P. Freitag, S. P. Hayes, B. A. Taft, Z. Chen and K. Wyrtki, 1988: The response of the equatorial Pacific Ocean to a westerly wind burst in May 1986. *J. Geophys. Res.,* **93,** 10 589–10 603.

Moore, D. W., 1979: Modelling the tropical ocean circulation. *Modèles Numériques de la Circulation Océanique.* J. J. O'Brien, Ed., Florida State University, Tallahassee.

Moum, J. N., and D. R. Caldwell, 1985: Local influences on shear-flow turbulence in the equatorial ocean. *Science,* **230,** 315–316.

Niiler, P. P., R. E. Davis and H. J. White, 1987: Water-following characteristics of a mixed layer drifter. *Deep-Sea Res.,* **34,** 1867–1881.

Pacanowski, R., and S. G. H. Philander, 1981: Parameterization of vertical mixing in numerical models of tropical oceans. *J. Phys. Oceanogr.,* **11,** 1443–1451.

Peters, H., M. C. Gregg and J. M. Toole, 1988: On the parameterization of equatorial turbulence. *J. Geophys. Res.,* **93,** 1199–1218.

Richman, J. G., R. A. de Szoeke and R. E. Davis, 1987: Measurement of near-surface shear in the ocean. *J. Geophys. Res.,* **92,** 2851–2858.

Schneider, N., and P. Müller, 1990: The meridional and seasonal structures of the mixed-layer depth and its diurnal amplitude observed during the Hawaii-to-Tahiti Shuttle Experiment. *J. Phys. Oceanogr.* submitted.

Smith, J. D., 1974: Turbulent structure of the surface boundary layer in an ice-covered ocean. *Rapp. P.-v. Rùn. Cons. int. Explor. Mer.,* **167,** 53–65.

Spain, P. F., D. L. Dorson and H. T. Rossby, 1981: Pegasus: A simple, acoustically tracked velocity profiler. *Deep-Sea Res.,* **28A,** 1553–1567.

Stommel, H., 1960: Wind-drift near the Equator. *Deep-Sea Res.,* **6,** 298–302.

Thorade, H., 1914: Die Geschwindigkeit von Triftstromungen und die Ekmanshe Theorie. *Ann. d. Hydrogr. u. Mar. Meteor.,* **42,** 379–391.

Wyrtki, K., E. Firing, D. Halpern, R. Knox, G. J. McNally, W. C. Patzert, E. D. Stroup, B. A. Taft and R. Williams, 1981: The Hawaii to Tahiti Shuttle Experiment. *Science,* **211,** 22–28.